Capturing non-linear stress-strain response of brittle rocks due to closure of coring-induced micro-cracks using 3D bonded block model

Conference Paper · June 2020

2 authors:

Navid Bahrani
Dalhousie University

Benoît Valley
Université de Neuchâtel

ARMA 20–1471

Capturing non-linear stress-strain response of brittle rocks due to closure of coring-induced micro-cracks using 3D bonded block model

Bahrani, N.
Dalhousie University, Halifax, NS, Canada
Valley, B.
University of Neuchâtel, Neuchâtel, Switzerland

ABSTRACT: The stress-strain curves of brittle rocks can be divided into five regions: 1. crack closure, 2. elastic region, 3. crack initiation, 4. crack damage, and 5. peak and post-peak region. The initial non-linear section of the stress-strain curve is known to be due to the closure of pre-existing micro-cracks. This non-linear section may or may not be present depending on the density and geometry of pre-existing micro-cracks. It is known that some of these micro-cracks may form due to the stress redistribution and tensile stresses generated inside the cores during drilling from deep and high stress grounds. The presence of such micro-cracks may affect the properties of rock specimens determined from laboratory tests. Therefore, the knowledge of the level of core damage (micro-crack density) and associated changes in the laboratory properties of brittle rocks is of paramount importance for reliable designs of deep underground excavations. In this paper, the discontinuum numerical program 3DEC and its Bonded Block Model (BBM) is used to explicitly simulate drilling-induced core damage. The laboratory test data from the well documented case of the AECL's Underground Research Laboratory (URL) is used for numerical simulation and model calibration. The numerical simulations involve: 1) calibrating a 3D BBM to the properties of undamaged Lac du Bonnet (LdB) granite under an unconfined condition, 2) simulating core drilling and associated micro-cracks in the cored specimen (i.e., BBM), and 3) uniaxially loading the damaged BBM and comparing its mechanical properties with those of damaged LdB granite. It is found that the initial region of the stress-strain curve of the damaged BBM is non-linear. This is interpreted to be due to the closure of micro-cracks generated during core drilling simulation. The results of numerical study presented in this paper demonstrate the capability of the proposed modeling approach for a realistic simulation of drilling-induced core damage and associated non-linear stress-strain response of brittle rocks.

1. INTRODUCTION

Rock mechanics parameters such as the Unconfined Compressive Strength (UCS) and the elastic modulus (E) are required at different design stages of deep engineering projects such as deep mines and nuclear waste repositories, and those requiring fluid flow at depth for the energy sector (e.g., oil and gas, deep geothermal, CO2 sequestration). The procedure to determine these properties is to perform standard rock mechanics laboratory tests on cored samples. The process of core drilling may induce damage in the form of micro-cracks to the cored samples particularly in deep operations, where the cores experience complex stress path, large stress relief and high tensile stresses during drilling. This raises a question of whether the mechanical properties of damaged specimens determined from laboratory tests are representative of those in situ.

This paper presents the results of a three-dimensional (3D) numerical study that attempted to simulate drilling-induced core damage and associated non-linear stress-strain response of brittle rocks due to the closure of micro-cracks in unconfined compression tests. The numerical program 3DEC (by Itasca) and its bonded block modelling methodology (Garza-Cruz et al., 2014) is used for this purpose. The laboratory test data from the well documented case of the AECL's Underground Research Laboratory (URL) is used for model calibration. The procedure for simulating core drilling processes as well as challenges involved in matching the macro properties of numerical specimens to those of undamaged and damaged Lac du Bonnet granite specimens are discussed in detail. The outcome of this research is a step towards a more realistic simulation of core damage, potentially offering a tool to help derive relevant rock mechanics design parameters for deep engineering projects.

2. EVIDENCE OF DRILLING-INDUCED CORE DAMAGE AT THE URL

Fracturing in brittle rocks is a complex process. It is known that the presence of grain-scale heterogeneities in brittle rocks results in progressive fracturing, which initiates at about 40-60% of the peak stress (Hoek and Martin, 2014). Figure 1 shows that the stress-strain response of brittle rocks is typically divided into five regions: 1. crack closure, 2. elastic region, 3. crack initiation, 4. crack damage, and 5. peak and post-peak region. The initial non-linear region of the stress-strain curve is known to be due to the closure of pre-existing micro-cracks. This non-linear section may or may not be present in the rock specimens depending on the initial micro-crack density and geometry. Some of these micro-cracks may be natural, some may develop during sample preparation (near the ends of the specimen), and some may form during drilling from deep and high stress grounds due to the stress redistribution and tensile stresses generated inside the core.

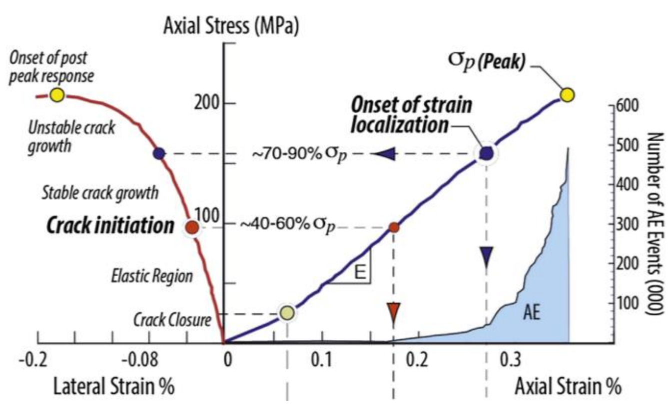

Fig. 1. Stages in progressive failure of intact rock specimens subjected to compressive loading (after Hoek and Martin, 2014)

Evidence of sample disturbance (i.e., core damage) at the Canada's Underground Research Laboratory (URL) has been reported by Martin and Stimpson (1994) and Eberhardt et al. (1999). Martin and Stimpson (1994) observed a decrease in the values of UCS, Young's modulus and acoustic velocity of LdB granite specimens with increasing depth due to the drilling-induced core damage. Martin and Stimpson (1994) identified three stress domains at the URL; Domain 1 which extends from surface to a depth of 200 m, Domain 2 at 240 m Level, and Domain 3 at 420 m Level. As demonstrated in Figure 2a, no sample disturbance was encountered in Domain 1, however, samples retrieved from Domain 2 and Domain 3 were partially and severely damaged, respectively.

Another indication of core damage in the samples retrieved from Domain 3 is the initial non-linear response of the stress-strain curve under unconfined compression. Figure 2b shows that the undamaged sample retrieved from near surface (i.e. Domain 1) responds in a linear elastic manner, whereas damaged sample from Domain 3 initially exhibits a strongly non-linear response due to the closure of micro-cracks. These observations were consistent with the results of the SEM analyses by Eberhardt et al. (1999), who noted that visible cracks were difficult to find in the thin sections of the samples from the 130 m and 240 m Levels, whereas numerous cracks were visible in the samples retrieved from the 420 m Level.

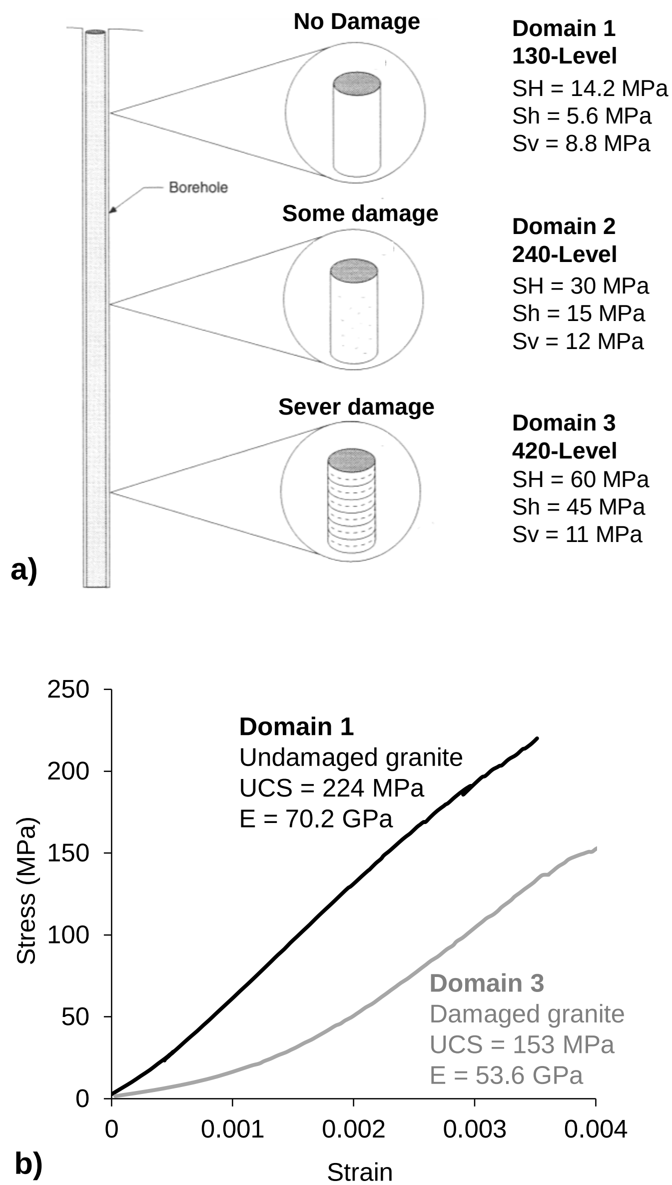

Fig. 2. a) Observed sample disturbance as a function of depth at the URL (after Martin and Stimpson, 1994); b) stress-strain response of LdB granite samples retrieved from Cold Spring Quarry (Domain 1) and 420 m level (Domain 3) (Courtesy of Dr. Derek Martin)

The drilling-induced core damage has been studied by several researchers using continuum (Li and Schmitt, 1997; Corthésy and Leite 2008; Valley et al., 2010a) and discontinuum (Bahrani et al., 2015; Wu et al., 2018) models. However, only few have explicitly simulated this phenomenon using full 3D discontinuum models (e.g., Holt et al., 2003; Wu et al., 2018). Two important factors need to be considered when using numerical models to realistically simulate core damage initiation and accumulation processes: 1) grain-scale heterogeneities due to grain shapes and geometrical arrangements (Bewick et al., 2012) as well as the stiffness contrast between mineral grains (Valley et al., 2010b); 2) complex 3D coring stress path (Bahrani et al., 2015; 2019). The former results in the generation of local tensile stresses and associated cracks at an overall stress that is much lower than the peak strength, and the latter results in the progressive initiation and accumulation of cracks inside the core at different orientations relative to the core axis.

Several attempts have been made to capture the initial non-linear section of the stress-strain curve in brittle rocks due to the closure of pre-existing cracks using discontinuum numerical models. The results of numerical simulations by Bahrani et al. (2015) and Hamdi et al. (2015) demonstrated that although an addition of micro-cracks to the numerical specimen may result in the reduction in the values of UCS and elastic modulus, capturing the crack closure section of the stress-strain curve requires the presence of open cracks that are gradually closed during uniaxial loading. The crack closure behavior of rocks in compression has been successfully captured in PFC by Ji et al. (2018) who simulated pre-existing open cracks by debonding some of the contacts and opening them by introducing two notional surfaces and giving them a negative reference gap.

3. BONDED BLOCK MODEL OF LAC DU BONNET GRANITE

3DEC was used to simulate the process of core drilling and associated core damage observed at three stress domains at the URL. For this purpose, a laboratory-scale rock specimen was first simulated in 3DEC by dividing the model into several tetrahedral blocks bonded together at their triangular faces (contacts). This model is referred to as the Bonded Block Model (BBM) (Garza-Cruz et al., 2014).

The BBM has been used to simulate the failure processes of brittle rocks at different scales in UDEC (e.g., Gao and Stead, 2014; Sinha and Walton, 2019) and 3DEC (e.g., Garza-Cruz et al., 2014; Ghazvinian et al., 2014). When used to simulate laboratory-scale rock specimens, the BBM is also referred to as the Grain-based Model (GBM) (Lan et al., 2010; Wang and Cai, 2018; Sinha and Walton, 2020). In this regard, blocks and contacts serve as grains and grain boundaries, respectively. The blocks (grains) can be assumed to be elastic or inelastic (Sinha and Walton, 2020), or divided into a number of smaller blocks. In the latter approach, intra-grain fracturing can be explicitly simulated (Wang and Cai, 2018). The grain boundaries (contacts) are usually assigned Mohr-Coulomb strength properties with brittle or strain softening post-peak response (Lan et al., 2010; Wang and Cai, 2018; Sinha and Walton, 2020).

A 5 cm × 10 cm cylindrical specimen was generated in 3DEC and then converted to a BBM consisting of 9895 blocks (Fig. 3a). The size and therefore the number of blocks in the BBM was selected in order to ensure that there are at least 10 blocks (grains) across the diameter of the numerical specimen (Fig. 3b).

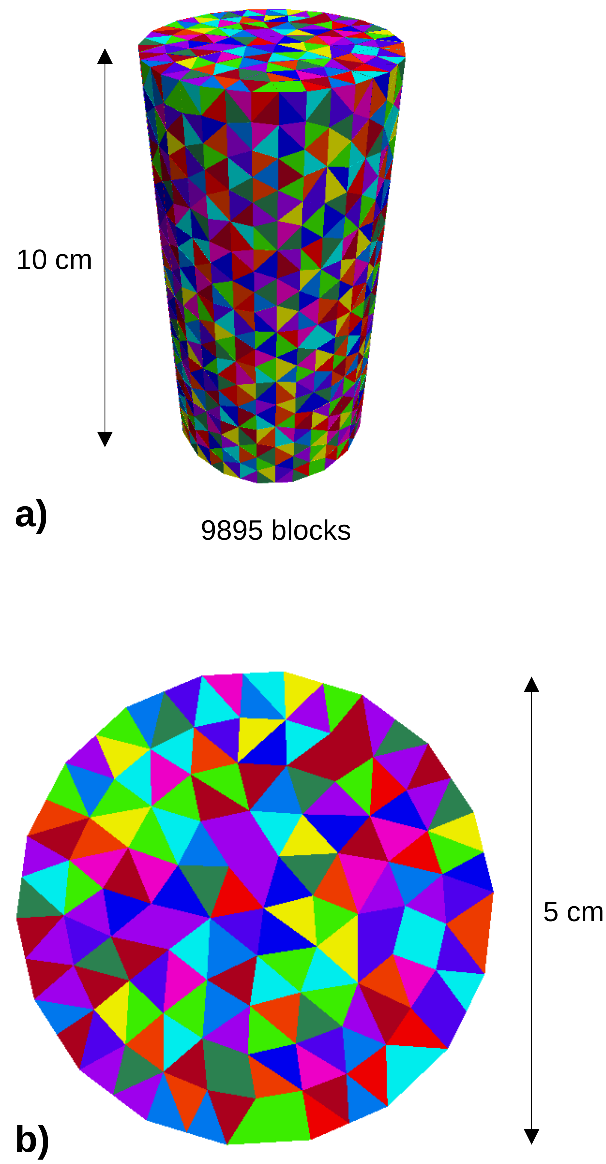

Fig. 3. Generated BBM in 3DEC: b) side view and b) top view

The UCS test was simulated by applying a constant vertical velocity to the top boundary of the specimen while the bottom boundary was fixed in the vertical direction. The simulation of the direct tensile test was carried out by applying a constant vertical velocity to the top and bottom model boundaries in opposite directions.

The axial stress was calculated by averaging the axial stress in the zones of blocks whose centroids fell within a 1 cm × 1 cm × 1 cm cube in the center of the specimen, following the approach used by Ghazvinian et al. (2014). The axial strain was calculated from the displacement of a grid point in the center of the top boundary of the specimen.

The BBM calibration was conducted with respect to the average UCS, direct tensile strength and elastic modulus of undamaged LdB granite. To reduce the computation time, several assumptions were made for the properties of the blocks (grains) and contacts (grain boundaries). For example, the grains were simulated as elastic blocks, forcing the failure to occur only at the grain boundaries. Furthermore, one mineral grain type was used in the BBM, and all the grain boundaries were assigned the same properties.

The BBM calibration was initiated by adjusting the contact peak tensile strength to match the direct tensile strength of undamaged LdB granite. The BBM was then calibrated to the UCS of undamaged LdB granite by adjusting the contact peak cohesion, and to its Young's modulus by adjusting the block elastic modulus and contact stiffness (normal and shear) properties. Table 1 lists the micro-properties obtained from this calibration process. The simulation results presented in Table 2 show an agreement between macro-properties of the calibrated BBM and laboratory properties of undamaged LdB granite.

Table 1. Micro-properties of BBM calibrated to laboratory properties of undamaged LdB granite

Block (grain) properties	Young's modulus (GPa)	75 GPa
	Poisson's ratio	0.22
Contact (grain boundary) properties	Normal stiffness (GPa/m)	50,000
	Shear stiffness (GPa/m)	20,000
	Peak tensile strength (MPa)	13
	Residual tensile strength (MPa)	0
	Peak cohesion (MPa)	140
	Residual cohesion (MPa)	0
	Peak friction angle (°)	0
	Residual friction angle (°)	30

Table 2. Comparison between laboratory properties of undamaged LdB granite and macro-properties of calibrated BBM

Parameters	Intact LdB granite	Undamaged BBM
UCS (MPa)	213 ± 20	211
σ_t (MPa)	7 ± 1	8.5
E (GPa)	65 ± 5	68

Figure 4 and Figure 5 present the stress-strain curves and failure modes from the unconfined compressive and direct tensile tests simulated on the calibrated BBM. The failure modes of the BBM were found to be consistent with those observed in the laboratory. In the UCS test (Fig. 4), cracking in the BBM initiated at an axial stress of 70 MPa, which is about 30% of the peak strength. At the peak stress, the cracks were randomly distributed inside the specimen. In the direct tensile test (Fig. 5), cracking initiated at about 85% of the peak stress, and then propagated just past the peak stress to generate a single fracture perpendicular to the specimen axis. In the next section, the calibrated BBM is used as part of a larger 3DEC model to explicitly simulate drilling-induced core damage.

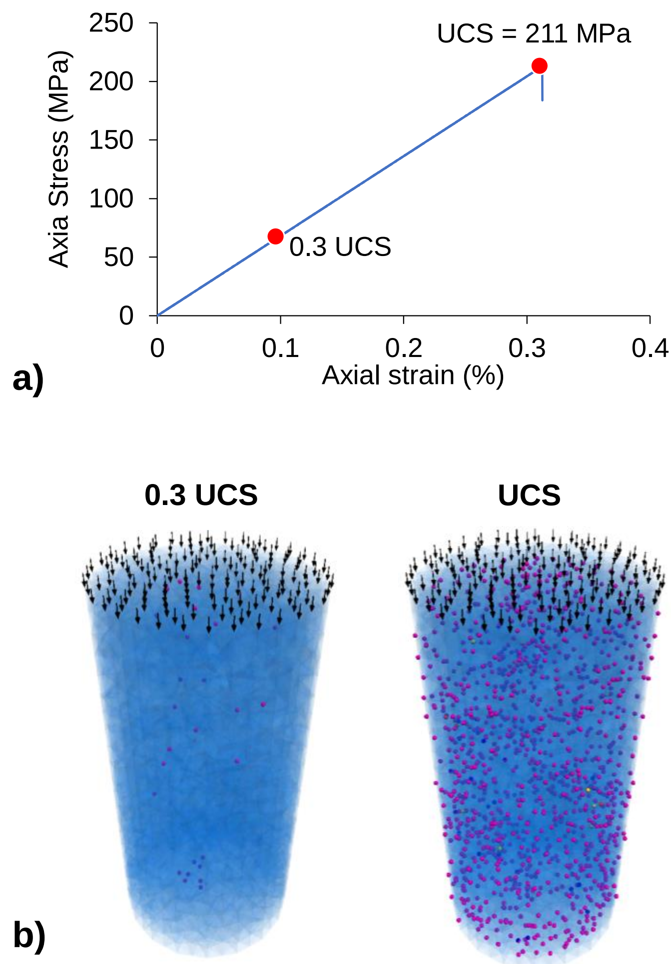

Fig. 4. Results of BBM calibrated to laboratory properties of undamaged LdB granite: a) stress-strain curve under unconfined compression; and b) contact failure at 30% of the UCS (left image) and the UCS (right image).

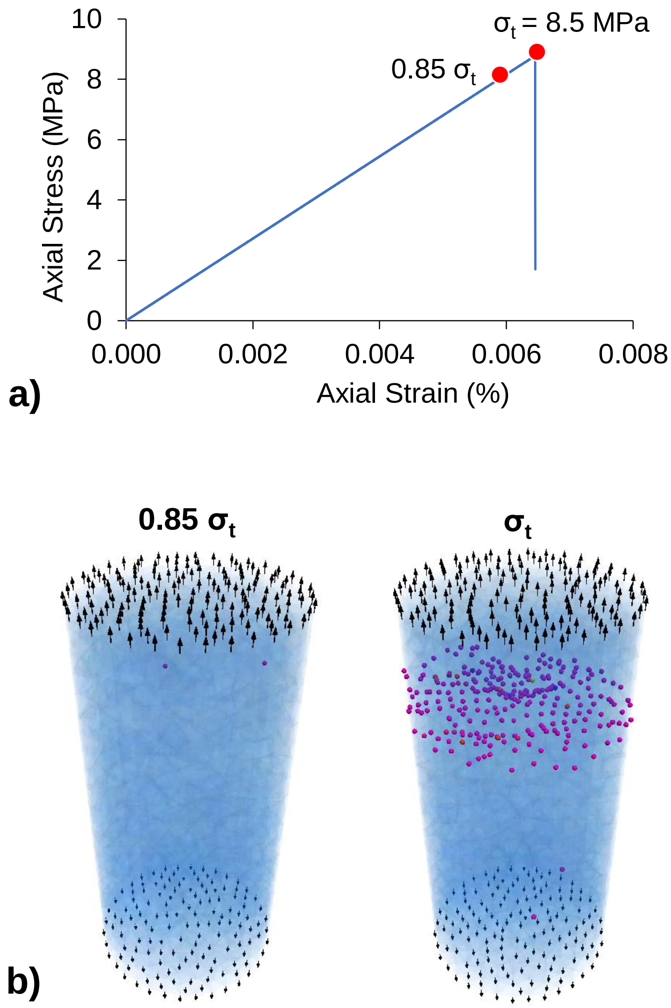

Fig. 5. Results of BBM calibrated to laboratory properties of undamaged LdB granite: a) stress-strain curve under direct tension; and b) contact failure at 85% of the peak tensile strength (left image) and the peak tensile strength (right image)

4. SIMULATION OF CORE DRILLING AND ASSOCAITED CORE DAMAGE

In the next step, 3DEC was used as a coupled continuum-discotinumm model to explicitly simulate the drilling process and associated core damage observed at the URL. In this modelling approach, 3DEC is usually divided into two domains: continuum and discontinuum. The discontinuum domain is used to explicitly capture the brittle damage. The continuum domain allows for elastic stresses to redistribute far from the excavation, where brittle damage or failure is not expected (Bahrani and Hadjigeorgiou, 2018).

In the present study, the discontinuum domain is the calibrated BBM, which represents a section of the core where micro-cracking is explicitly simulated. The BBM, with micro-properties provided in Table 1, is embedded in a 60 cm × 60 cm × 60 cm continuum model with elastic properties of undamaged LdB granite. Figure 6a shows the geometry of the 3DEC model, including the core in the continuum and discontinuum domains, with a total length of 55 cm. Several excavation stages were used to capture the progressive drilling process. The simulation of core drilling starts from one side of the 3DEC model. The first 30 cm of the core is inside the continuum domain. The core length in the discontinuum domain (BBM) is 10 cm. The drilling in this domain is simulated in 10 excavation stages with 1 cm drilling advance per stage. After the BBM is cored, the drilling simulation continues in the continuum domain with a length of 15 cm. Figure 6b shows a closer view of the core in the discontinuum domain before and after drilling.

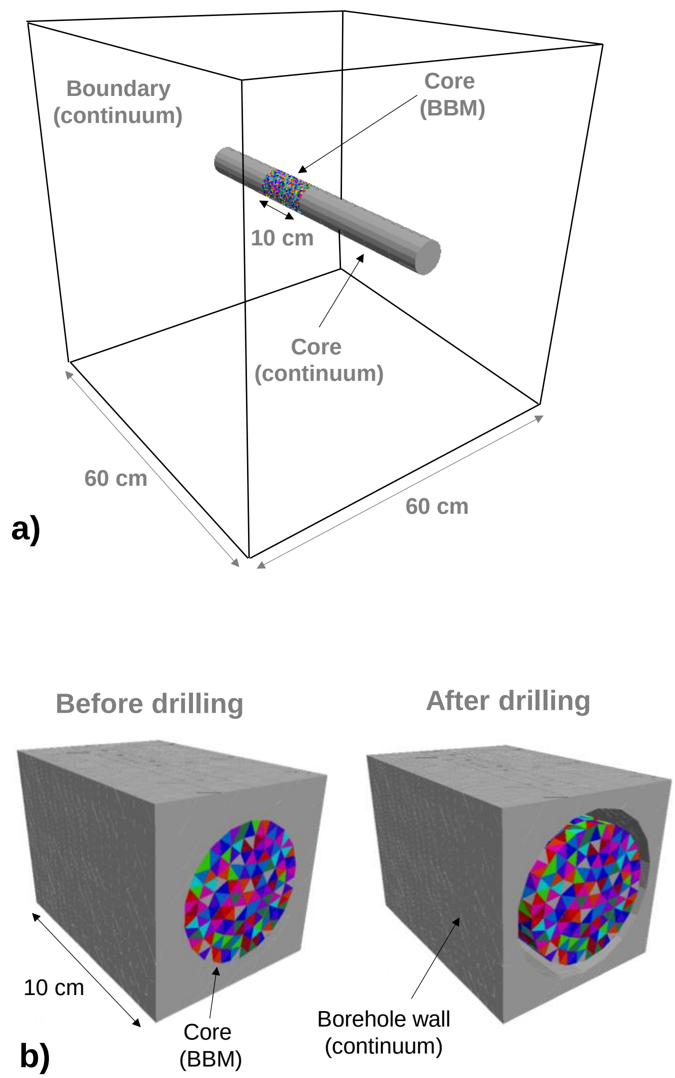

Fig. 6. a) 3DEC model showing the core in the continuum and discontinuum domains; and b) BBM representing the core before and after drilling

Core drilling simulations were carried out for three stress domains at the URL. The boreholes were assumed to be vertical, therefore, aligned with the vertical stress component (Sv). Figure 7 shows the simulated core damage (failed contacts in BBM) following the completion of drilling simulation for three stress domains. The simulation results indicate that the amount of core damage (micro-crack density) increases with depth from Domain 1 to Domain 3. In Domain 1, no damage is observed inside the core, while sporadic failed contacts appear at the outer surface of the core. In Domain 2, more systematic damage can be seen at the core boundary. The core in Domain 3 is heavily damaged. By comparing Figure 7 and Figure 2a, it is concluded that the proposed coupled continuum-discontinuum numerical modeling approach can qualitatively capture the drilling-induced core damage observed at different stress domains at the URL.

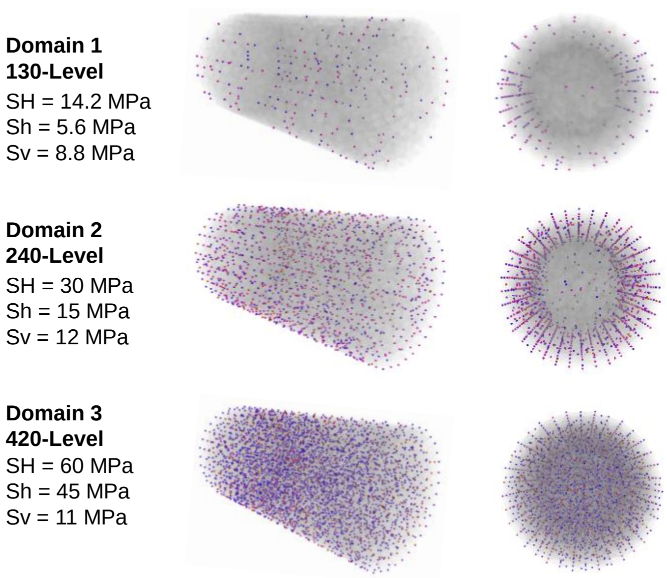

Fig. 7. Simulated core damage (failed contacts) in BBM at three stress domains at the URL

5. SIMULATION OF UCS TEST ON DAMAGED CORE

In order to evaluate the influence of core damage on the laboratory properties of cored samples and to investigate whether the crack-closure region of the stress-strain curve can be captured in 3DEC, an unconfined compression test was simulated on the damaged BBM from Domain 3. For this purpose, the continuum section of the 3DEC model was first deleted following the completion of the core drilling simulation. The UCS test was then simulated on the damaged BBM following the procedure described in Section 3.

The stress-strain curves of the undamaged and damaged BBMs (called BBM1 here) are presented in Figure 8. As can be seen in this figure, the damaged BBM1 exhibits a strong non-linear behavior at early stages of uniaxial loading. This initial non-linear response is due to the closure of the micro-cracks (failed contacts) generated during the drilling simulation. The UCS and elastic modulus of the damaged BBM1 are 78.2 MPa and 51.2 GPa, respectively, and are lower than those of the undamaged BBM1. Although the elastic modulus of the damaged BBM1 matches that of damaged LdB granite determined from laboratory tests, its UCS underestimates that of damaged LdB granite by a factor of about 2 (the average UCS of damaged LdB granite is about 157 MPa; Martin and Stimpson, 1994; Eberhardt et al., 1999). The macro-properties of damaged LdB granite and BBM1 are compared in Table 3.

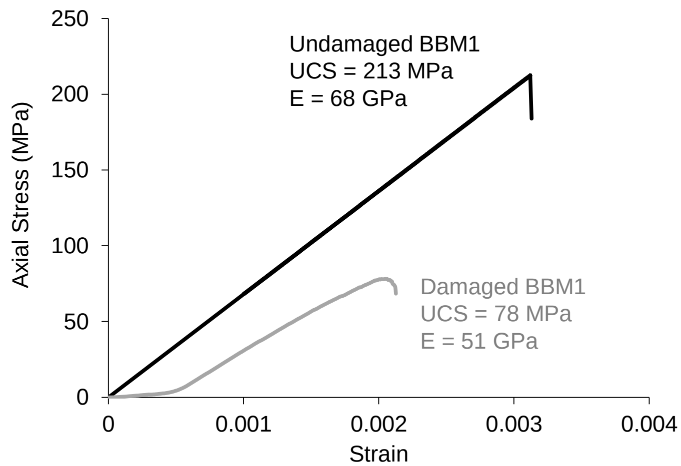

Fig. 8. Comparison between the stress-strain curves of undamaged and damaged BBMs1 calibrated to the properties of undamaged LdB granite

Table 3. Comparison between laboratory properties of damaged LdB granite and macro-properties of damaged BBM1

Parameters	Damaged LdB granite	Damaged BBM1
UCS (MPa)	157.9 ± 17.7	78
E (GPa)	51.9 ± 1.6	51

The underestimation of the UCS of damaged LdB granite by the BBM1 calibrated to the properties of undamaged LdB granite could be due to the following reasons:

a) The level of core damage (i.e., density of coring-induced micro-cracks) is too high following the simulation of core drilling;

b) The residual strength of the failed contacts (i.e., residual friction angle) is too low.

Therefore, in order to match the properties of both undamaged and damaged BBMs to those of LdB granite, the BBM1 had to be re-calibrated. For this purpose, an iterative calibration procedure similar to that proposed by Bahrani et al. (2011; 2015) was used. This calibration process involved the following general three steps:

1) Calibration of BBM to the properties of undamaged LdB granite: The BBM was re-calibrated to the uniaxial compressive and tensile strengths as well as the elastic modulus of undamaged LdB granite by

adjusting the residual friction angle, the cohesion, the tensile strength, and the normal and shear stiffness values of the contacts.

2) Simulation of core drilling and associated core damage: Core drilling was simulated following the procedure described in Section 5. The BBM representing the core was assigned the micro-properties obtained from Step 1, and the core drilling simulation was conducted with the in-situ stress state representative for Domain 3.

3) UCS test simulation on damaged BBM: The continuum domain of the coupled continuum-discontinuum 3DEC model was deleted, and the UCS test was simulated on the damaged BBM. The peak strength and elastic modulus of the damaged BBM were compared with those of damaged LdB granite. If a match with the properties of damaged LdB granite was not achieved, model calibration had to be redone from Step 1.

After several attempts to calibrate the BBM to the properties of both undamaged (intact) and damaged LdB granite, it was found that it is not possible to obtain both the peak strength and the Young's modulus of the damaged LdB granite in a single BBM. This means that either the peak strength or the elastic modulus in one BBM could be matched with those of damaged LdB granite, but not both. Table 4 provides a comparison between the laboratory properties of undamaged and damaged LdB granite and the macro-properties of BBMs obtained from two calibration attempts (called BBM2 and BBM3 here) following the procedure described above.

Table 4. Comparison between laboratory properties of undamaged and damaged LdB granite and those of BBM2 second calibration attempt) and BBM3 (third calibration attempt)

Laboratory properties of LdB granite		
Parameter	Undamaged	Damaged
UCS (MPa)	213 ± 20	157.9 ± 17.7
E (GPa)	65 ± 5	51.9 ± 1.6
Macro-properties of BBM2		
Parameter	Undamaged	Damaged
UCS (MPa)	206.4	156.4
E (GPa)	68.1	64
Macro-properties of BBM3		
Parameter	Undamaged	Damaged
UCS (MPa)	216.5	120
E (GPa)	65.4	55

The stress-strain curves of both undamaged and damaged BBM2 and BBM3 are presented in Figure 9. As can be seen in this figure, both damaged BBMs show a non-linear response at the early stages of uniaxial loading. Note that the stress-strain curves of the undamaged BBMs are linear, and their macro-properties match those of intact LdB granite. Figure 9a shows that the damaged BBM2 calibrated to the peak strength of damaged LdB granite overestimates the Young's modulus of damaged LdB granite. In Figure 9b, the damaged BBM3 calibrated to the Young's modulus of damaged LdB granite underestimates the UCS of damaged LdB granite.

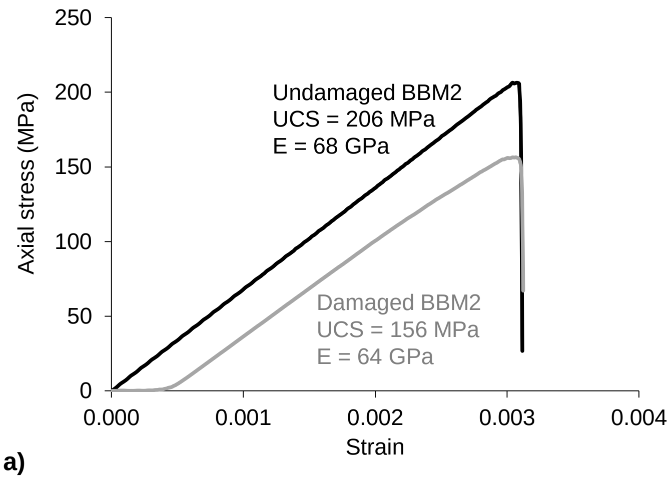

a)

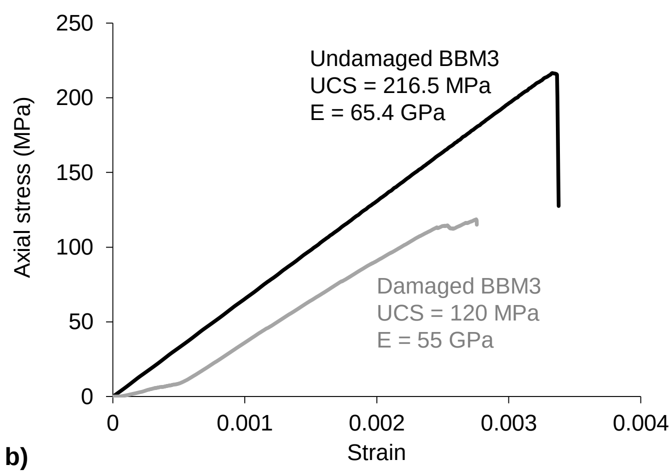

b)

Fig. 9. Stress-strain curves of two BBMs: a) re-calibrated to the UCS of damaged LdB granite (Young's modulus of damaged LdB granite is overestimated); and b) re-calibrated to the Young's modulus of damaged LdB granite (UCS of damaged LdB granite is underestimated)

The micro-properties of both BBMs obtained from the iterative calibration procedure described above are provided in Table 5. The comparison between the micro-properties of both BBMs reveals that the main difference between the two models is the contact normal and shear stiffness values; the stiffness properties of the BBM3 matched the Young's modulus (but underestimated the UCS) of damaged LdB granite are lower than those of the BBM2 matched the UCS (but overestimated the Young's modulus) of damaged LdB granite.

Table 5. Micro-properties of BBM2 and BBM3

Micro-properties	Parameters	BBM2	BBM3
Block (grain)	Young's modulus (GPa)	75	75
	Poisson's ratio	0.22	0.22
Contact (grain boundary)	Normal stiffness (GPa/m)	50,000	35,000
	Shear stiffness (GPa/m)	20,000	14,000
	Peak tensile strength (MPa)	13	13
	Residual tensile strength (MPa)	0	0
	Peak cohesion (MPa)	115	115
	Residual cohesion (MPa)	0	0
	Peak friction angle (°)	0	0
	Residual friction angle (°)	50	52

Research is ongoing to more realistically capture the drilling-induced core damage and core disking observed at the URL and to improve the BBM calibration results in terms of the stress-strain response, the UCS, and the Young's modulus of both undamaged and damaged specimens.

6. CONCLUSIONS

In this paper, the Bonded Block Model (BBM) was used to simulate the core drilling and core damage observed at the AECL's Underground Research Laboratory (URL). It was found that the calibrated BBM can capture different levels of core damage observed at three stress domains at the URL. The results of numerical simulations demonstrated the capability of the proposed modeling approach for a realistic simulation of drilling-induced core damage and associated initial non-linear section of the stress-strain curve due to the closure of micro-cracks.

Different challenges in calibrating the BBM to the UCS and Young's modulus of both undamaged and damaged LdB granite were discussed in this paper. Several improvements to the proposed modeling approach are foreseen for future studies, e.g., the use of more realistic grain geometries (i.e., 3D Voronoi blocks) and the consideration of grain property heterogeneities (i.e., stiffness and strength). Following recent findings of Bahrani et al. (2019), the proposed modeling approach will be used to further investigate the influence of core damage on the results of core- and borehole-based in situ stress estimation techniques such as the overcoring, borehole breakout, and the Kaiser effect techniques.

ACKNOWLEDGEMENT

The authors wish to acknowledge Dr. Peter Kaiser for his contributions and many insightful discussions over the years and recently.

REFERENCES

Bahrani, N. & Hadjigeorgiou, J. 2018. Influence of stope excavation on drift convergence and support behavior - insights from 3D continuum and discontinuum models. *Rock Mechanics and Rock Engineering*, 51: 2395–2413.

Bahrani, N. Valley, B. Kaiser, PK. 2015. Numerical simulation of drilling-induced core damage and its influence on mechanical properties of rocks under unconfined condition. *International Journal of Rock Mechanics and Mining Sciences*, 80: 40-50.

Bahrani, N. Valley, B. Kaiser, PK. 2019. Influence of stress path on stress memory and stress fracturing in brittle rocks. *Canadian Geotechnical Journal*, 56(6): 852-867.

Bewick, RP. Valley, B. & Kaiser, PK. 2012. Effect of Grain Scale Geometric Heterogeneity on Tensile Stress Generation in Rock Loaded in Compression. *46th US Rock Mechanics/Geomechanics Symposium*, 24-27 June, Chicago, Illinois.

Corthésy, R. Leite, MH. 2008. A strain-softening numerical model of core discing and damage. *International Journal of Rock Mechanics and Mining Sciences*, 45: 329-50.

Eberhardt E. Stead D. & Stimpson B. 1999. Effects of sample disturbance on the stress- induced microfracturing characteristics of brittle rock. *Canadian Geotechnical Journal*, 36: 239-250.

Gao, F. Stead, D. 2014. The application of a modified Voronoi logic to brittle fracture modelling at the laboratory and field scale. *International Journal of Rock Mechanics and Mining Sciences*, 68:1-14.

Garza-Cruz, TV, Pierce, M & Kaiser, PK 2014, Use of 3DEC to study spalling and deformation associated with tunnelling at depth, 7*th International Conference on Deep and High Stress Mining*, Australian Centre for Geomechanics, Perth, pp. 421-434.

Ghazvinian, E. Diederichs, M. Quey, R. 2014. 3D random Voronoi grain-based models for simulation of brittle rock damage and fabric-guided micro-fracturing. *Journal of Rock Mechanics and Geotechnical Engineering*, **6**: 506–21.

Holt RM, Doornhof D, Kenter CJ. 2003. Use of discrete particle modeling to understand stress-release effects on mechanical and petrophysical behavior of granular rocks. In: Konietsky H,editor. *Numerical Modeling in Micromechanics via Particle Methods*. Lisse: Swers & Zeitlinger; pp.269-276.

Ji P. Zhang X. & Zhang A. 2018. A new method to model the non-linear crack closure behavior of rocks under uniaxial compression. *International Journal of Rock Mechanics and Mining Sciences*, 112: 171-183

Lan, H., Martin, C.D. and Hu, B. 2010. Effect of heterogeneity of brittle rock on micromechanical extensile behavior during compression loading. *Journal of Geophysical Research: Solid Earth*. 115(B1).

Li, Y. Schmitt, DR. 1997. Effects of Poisson's ratio and core stub length on bottomhole stress concentrations. *International Journal of Rock Mechanics and Mining Sciences*, 34: 761-73.

Martin, D. Stimpson, B 1994. The effect of sample disturbance on the laboratory properties of Lac du Bonnet granite. *Canadian Geotechnical Journal*, **31**: 692-702.

Sinha, S., Walton, G., 2020. A study on Bonded Block Model (BBM) complexity for simulation of laboratory-scale stress-strain behavior in granitic rocks. *Computers and Geotechnics*. 118: 103363.

Valley, B. Bahrani, N. & Kaiser PK. 2010a. Rock strength obtained from core samples and borehole instabilities – the effect of drilling induced damage, *Proc. EUROCK 2010*, Switzerland, 4 p.

Valley, B. Suorineni, FT. & Kaiser, PK. 2010b. Numerical analyses of the effect of heterogeneities on rock failure process. *44th US Rock Mechanics/Geomechanics Symposium*, 27-30 June, Salt Lake City, Utah.

Wang, X., Cai, M., 2018. Modeling of brittle rock failure considering inter- and intra-grain contact failures. *Computers and Geotechnics*. 101: 224–244.

Wu, S. Wu, H. Kemeny, J. 2018. Three-dimensional discrete element method simulation of core disking. *Acta Geophysica*, 66: 267-282.